We are IntechOpen, the world's leading publisher of Open Access books Built by scientists, for scientists

4,800
Open access books available

122,000
International authors and editors

135M
Downloads

Our authors are among the

154
Countries delivered to

TOP 1%
most cited scientists

12.2%
Contributors from top 500 universities

WEB OF SCIENCE™

Selection of our books indexed in the Book Citation Index in Web of Science™ Core Collection (BKCI)

Interested in publishing with us?
Contact book.department@intechopen.com

Numbers displayed above are based on latest data collected.
For more information visit www.intechopen.com

Chapter 7

Absorption of Acoustic Phonons in Fluorinated Carbon Nanotubes with Non-Parabolic, Double Periodic Band

Daniel Sakyi-Arthur, S. Y. Mensah, N. G. Mensah, Kwadwo A. Dompreh and R. Edziah

Additional information is available at the end of the chapter

http://dx.doi.org/10.5772/intechopen.78231

Abstract

We studied theoretically the absorption of acoustic phonons in the hypersound regime in Fluorine modified carbon nanotube (F-CNT) Γ_q^{F-CNT} and compared it to that of undoped single walled carbon nanotube (SWCNT) Γ_q^{SWCNT}. Per the numerical analysis, the F-CNT showed less absorption to that of SWCNT, thus $|\Gamma_q^{F-CNT}| < |\Gamma_q^{SWCNT}|$. This is due to the fact that Fluorine is highly electronegative and weakens the walls of the SWCNT. Thus, the π-electrons associated with the Fluorine causes less free charge carriers to interact with the phonons and hence changing the metallic properties of the SWCNT to semiconductor by the doping process. From the graphs obtained, the ratio of hypersound absorption in SWCNT to F-CNT at $T = 45\,K$ is $\frac{\Gamma_{(SWCNT)}}{\Gamma_{(F-CNT)}} \approx 29$ while at $T = 55\,K$, is $\frac{\Gamma_{(SWCNT)}}{\Gamma_{(F-CNT)}} \approx 9$ and at $T = 65\,K$, is $\frac{\Gamma_{(SWCNT)}}{\Gamma_{(F-CNT)}} \approx 2$. Clearly, the ratio decreases as the temperature increases.

Keywords: carbon nanotube, fluorinated, acoustic effects, hypersound

1. Introduction

Acoustic effects in bulk and low dimensional materials have attracted lots of attention recently. This is due to the need of finding coherent acoustic phonons for scientific applications as against the use of conventional direct current [1]. Materials such as homogenous semiconductors, superlattices (SL), graphene and carbon nanotubes (CNT) are good candidates for such studies due to their novel properties such as the high scattering mechanism, the high-bias mean-free path (l) and their sizes which enable strong electron-phonon interaction to occur in them resulting in acoustic phonon scattering. Acoustic waves through these materials are

characterized by a set of elementary resonance excitations and dynamic nonlinearity which normally leads to an absorption (or amplification), acoustoelectric effect (AE) [2], and acousto-magnetoelectric effect (AME) [3, 4]. The concept of acoustic wave amplification was first predicted in bulk materials [5], and later in n-Ge [6]. In SLs, Mensah et al. [7] studied hypersound absorption (amplification) and established its use as a phonon filter, and in [8], predicted the use of the SL as a hypersound generator which was confirmed in [1]. In Graphene, Nunes et al. [9] treated theoretically hypersound amplification, but Dompreh et al. [10] further proved that absorption also occurs in the material. Experimentally, Miseikis et al. [11] and Bandhu and Nash [12] have studied acoustoelectric effect in Graphene.

Carbon nanotubes (CNTs), on the other hand, are cylindrical hollow rod of graphene sheets whose electronic structures are determined by the localized π-electrons in the sp^2- hybridized bonds. Absorption (Amplification) of hypersound in undoped CNT has been carried out theoretically by Dompreh et al. [13, 14] and experimentally by [15, 16]. Other forms of research such as hot-electron effect [17], thermopower in CNT [18] have been carried out. Flourine-modified CNT (F-CNT) is off-late attracting a lot of scientific interest. This is attained by doping the CNT with Fluorine thus forming double periodic band CNT changing from metallic to semiconductor. As per the studies conducted by Jeon et al. [19], absorption in F-CNT is less than that of SWCNT but no studies have been done on the absorption of F-CNT in the hypersound regime. In this paper, the study of absorption of acoustic phonons in metallic SWCNT and F-CNT are theoretically studied. Here, the acoustic wave considered has wavelength $\lambda = 2\pi/q$, smaller than the mean-free path of the CNT and then treated as a packet of coherent phonons (monochromatic phonons) having a δ-function distribution as

$$N(k) = \frac{(2\pi)^3}{\hbar\omega_q v_s}\Phi\delta(k-q) \tag{1}$$

where k is the phonon wavevector, $\hbar$ is the Planck's constant divided by 2π, and Φ is the sound flux density, and ω_q and v_s are respectively the frequency and the group velocity of sound wave with wavevector q. It is assumed that the sound wave is propagated along the z-axis of the CNT.

This paper is organized as follows: In Section 2, the absorption coefficient for F-CNT and SWCNT are calculated. In Section 3, the final equations are analyzed numerically and presented graphically. Section 4 presents the conclusion of the study.

2. Theory

Fluorination plays a significant role in the doping process, as it provides a high surface concentration of functional groups, up to C_2F without destruction of the tube's physical structure. Doping is an easy, fast, exothermic reaction and the repulsive interactions of the Fluorine atoms on the surface debundles the nanotube, thus enhancing their electron dispersion [20]. **Figure 1** shows a one dimensional SWCNT doped with Fluorine atoms [21]. Consider a Fluorine modified

CNT (n, n) with the Fluorine atoms forming a one-dimensional chain. A nanotube of this nature is equivalent to a band with unit cell as shown in **Figure 2**, where b is the bond length (C-C) [22].

The width for the F-(n, n) tube equals n periods (with a periodic length of $3b$), and this unit cell contains $N = 4n - 2$ carbon atoms which is shown in **Figure 3** [22]. **Figure 3** shows the atomic numbering in the unit cell of the F-(n, n) nanotube. For a conjugated $\pi-$ system, in which there is alternation of single and double bonds along a linear chain, the Hückel matrix approximation is

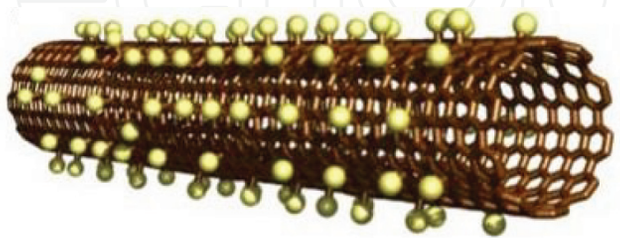

Figure 1. Fluorine modified SWCNT with the Fluorine atoms showing as yellow balls.

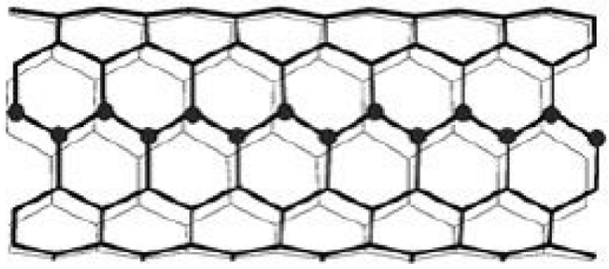

Figure 2. Fluorinated nanotube $F-(n,n)$ (dots denotes the positions of Fluorine atoms of Fluorine atoms that are covalently bonded to C atoms).

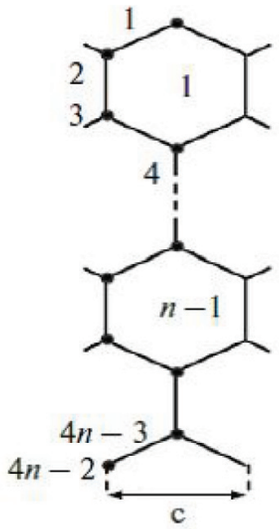

Figure 3. Atom numbering in the unit cells of nanotubes $F-(n,n)$.

employed to determine the electronic energy band. Proceeding as in [8, 23], we employ the Hamiltonian of the electron-phonon system in the FCNT in the second quantization formalism as

$$H = \sum_{p,\,\nu} \varepsilon^{(\nu)}(p)\left(p - \frac{e}{c}A(t)\right)a_p^{(\nu+)}a_\nu^{(\nu)} + \sum_k \omega_k b_k^+ b_k \ldots \\ + \frac{1}{\sqrt{N}}\sum_{p,\,k}\sum_{\nu\nu' n} c_k m_{\nu\nu'}(k_z)a_p^{(\nu+)}a_{p-k+ng}^{\nu'}\left(b_k^+ + b_{-k}\right) \tag{2}$$

where $\nu = 1, 2\ldots$ and for a chemically modified F-CNT, where the Fluorine atoms form a one-dimensional chain, the energy dispersion can be deduced by using the Huckel matrix method where translational symmetry is accounted for in [22] as

$$\varepsilon\left(p_z\right) = \varepsilon_o + \Xi_n\gamma_0\cos^{2N-1}\left(ap_z\right) \tag{3}$$

where $a = \sqrt{3}b/(2\hbar)$, Ξ is a constant, N is an integer, and ε_o is the minimum energy of the $\pi-$ electrons within the first Brillouin zone. For $N = 2$, the energy dispersion for F-CNT at the Fermi surface at the edge of the Brillouin zone is

$$\varepsilon\left(p_z\right) = \alpha_\pi + 8\gamma_o\cos^3\left(ap_z\right) \tag{4}$$

Eq. (4) can be expanded as

$$\varepsilon\left(p_z\right) = \varepsilon_o + \Delta_1\cos\left(3ap_z\right) + \Delta_2\cos\left(ap_z\right) \tag{5}$$

where ε_o is the electron energy in the first Brillouin zone with momentum p_o, i.e., $-\pi/a \leq p_o \leq \pi/a$, $\Delta_1 = \Delta/k_BT$, $\Delta_2 = 3\Delta/k_BT$ and $\Delta = 2\gamma_o$. By employing the coulombs gauge, the electromagnetic wave $E(t) = E_o\sin\omega t$ is related to the vector potential $A(t)$ is the vector potential related to the external electric field of the electromagnetic wave $E(t) = E_o\sin\omega t$ by the relation $E = -(1/c)(\partial A/\partial t)$ and is directed along the F-CNT tubular axis. $a_p^{(+)}$ and a_p are the creation and annihilation operators of an electron with quasi-momentum p in the νth miniband respectively, and b_k^+ and b_k are the phonon creation and annihilation operators respectively. N is the number of FCNT periods, $g = (0, 0, 2\pi/d)$ is the FCNT reciprocal vector, and $m_{\nu\nu'}$ is given by

$$m_{\nu\nu'}(k_z) = \int \varphi_{\nu'}^*(z)\varphi_\nu(z)e^{ik_z}dz \tag{6}$$

where $\varphi_\nu(z)$ is the wavefunction of the νth state in one of the one-dimensional potential wells from which the FCNT potential is formed. The electromagnetic wave frequency is assumed to be large compared with the inverse of the electron mean free time $1/\tau$ and the wavelength is taken to be large compared with the FCNT period, electron mean free path and the de Broglie wavelength. This opens the way for us to use the dipole approximation as in [8]. Moreover, the plane electromagnetic wave of frequency ω satisfies $\omega/\omega_p > 1$, where ω_p is the plasma frequency. In the case of the phonons, we confine our considerations to those for which the wavevector $\mathbf{q}$, satisfies the conditions $ql \gg 1$ where l is the electron mean free path in FCNT. Such phonons constitute a well-defined elementary excitations of the system.

For $\omega\tau \gg 1$ and $\omega > \omega_p$, ensures that the electromagnetic wave penetrate the sample and the condition $ql \gg 1$ means that the hypersound wavelength is far smaller than the electron mean free path. The phonon dispersion relation then reads as

$$i\frac{\partial}{\partial t}\langle b_q\rangle_t = \langle [b_q, H]\rangle_t = \omega_q \langle b_q\rangle_t + \frac{1}{\sqrt{N}} C_{-q} \sum_p m_{ss'}(-q_z)\left\langle a_p^{(s+)} a_{p+qng}^{(s)}\right\rangle_t \tag{7}$$

After much simplification, the phonon transition rate in the presence of the electromagnetic reduces to

$$\Gamma(q) = -Im\,\Omega = \frac{2\pi\Phi}{\omega_q V_s} \sum_{p_z,\, n'} \sum_{\ell=-\infty}^{\infty} J_\ell^2(\xi)$$

$$\times \left[f\left(\varepsilon_{n'}(p_z)\right) - f\left(\varepsilon_{n'}(p_z + \hbar q)\right)\right]\delta\left(\varepsilon_{n'}(p_z + \hbar q) - \varepsilon_{n'}(p_z) - \hbar\omega_q - \ell\Omega\right) \tag{8}$$

that is, the imaginary part of the polarization vector. In Eq. (8) $J_\ell(x)$ is the Bessel function of order ℓ and argument x. It follows from Eq. (8) that if $\Gamma(q) > 0$ we have hypersound attenuation, whereas if $\Gamma(q) < 0$ we have hypersound amplification due to absorption $\Gamma(q) > 0$ and emission $\Gamma(q) < 0$ of $|\ell|$ photons from the intensified laser field.

In the region of an intense laser field, i.e., $\xi \gg \omega$, only the electron-phonon collisions with the absorption or emission of $\ell \gg 1$ photons are significant. Accordingly, in the case of $\xi \gg \omega$ the argument of the Bessel function $J_\ell(\xi)$ is large. For large values, the Bessel function $J_\ell(\xi)$ is small except when the order is equal to the argument.

$$\xi = \frac{eE_o a^2 \Delta q}{\Omega^2} \tag{9}$$

Taking the sum over $|\ell|$ using the approximation in Eq. (10)

$$\sum_{\ell=-\infty} J_\ell^2(\xi)\delta(E - \ell\Omega) \approx \frac{1}{2}[\delta(E - \xi) + \delta(E + \xi)] \tag{10}$$

where $E = \varepsilon(p_z + \hbar q) - \varepsilon(p_z) - \hbar\omega_q$. Using the Fermi Golden Rule, the phonon transition rate reduces $\Gamma(q) = U_{n,n'}^{ac}$ where

$$U_{n,n'}^{ac} = \frac{2\pi\Phi}{\omega_q V_s} \sum_{p_z,\, p_z'} \sum_{n,\, n'} \Big\{ \left|G_{p_z - \hbar q,\, p_z}\right|^2 \left[f\left(\varepsilon_n(p_z - \hbar q)\right) - f\left(\varepsilon_n(p_z)\right)\right]\delta\left(\varepsilon_n(p_z - \hbar q) - \varepsilon_n(p_z) + \hbar\omega_q - \xi\right)$$

$$+ \left|G_{p_z + \hbar q,\, p_z}\right|^2 \left[f\left(\varepsilon_{n'}(p_z + \hbar q)\right) - f\left(\varepsilon_{n'}(p_z)\right)\right]\delta\left(\varepsilon_{n'}(p_z + \hbar q) - \varepsilon_{n'}(p_z) - \hbar\omega_q + \xi\right)\Big\} \tag{11}$$

$f(p_z) = f\left(\varepsilon_{n,n'}(p_z)\right)$ is the unperturbed distribution function, $\varepsilon_{n,n'}(p_z)$ is the energy band, n and n' denotes the quantization of the energy band, and $G(p_z \pm \hbar q, p_z)$ is the matrix element of the electron-phonon interaction. Letting $p_z' = p_z \pm \hbar q$ and employing the principle of detailed balance, we assume that scattering into a state p_z' and out of the state p_z is the same, and hence

$$\left|G_{p',p}\right|^2 = \left|G_{p,p'}\right|^2 \tag{12}$$

Substituting Eq. (12) into Eq. (11) and also converting the summation over $p_z^{'}$ into an integral, we obtain

$$\Gamma(q) = \frac{2\pi\Phi}{\omega_q v_s}.\sum_{n,\,n'}\left|G_{p',p}\right|^2\int\left[f\left(\varepsilon\left(p_z\right)\right) - f\left(\varepsilon\left(p_z+\hbar q\right)\right)\right]\delta\left(\varepsilon_{p_z+q} - \varepsilon_{p_z} - \hbar\omega_q + \xi\right)dp_z \tag{13}$$

The matrix element of the electron-phonon interaction is given as

$$\left|G_{p',p}\right| = \frac{\Lambda q}{\sqrt{2\sigma\omega_q}} \tag{14}$$

where Λ is the deformation potential constant, and σ is the density of F-CNT. Substituting Eq. (14) into Eq. (13), we obtain

$$\begin{aligned}\Gamma(q) = \frac{2\pi\Phi}{\omega_q v_s}\left(\frac{\Lambda q}{\sqrt{2\sigma\omega_q}}\right)^2\sum_{n,\,n'}\left[f\left(\varepsilon_{n'}\left(p_z\right)\right) - f\left(\varepsilon_{n'}\left(p_z+\hbar q\right)\right)\right] \\ \times\,\delta\left(\varepsilon_{n'}\left(p_z+\hbar q\right) - \varepsilon_{n'}\left(p_z\right) - \hbar\omega_q + \xi\right)dp_z\end{aligned} \tag{15}$$

The electron distribution function is obtained by obtained by solving the Boltzmann transport equation in the presence of external electric field

$$\frac{\partial f(r,p,t)}{\partial t} + v(p).\nabla_r f(r,p,t) + eE\nabla_p f(r,p,t) = -\frac{f(r,p,t) - f_o(p)}{\tau} \tag{16}$$

and has a solution of

$$f\left(p_z\right) = \int_0^\infty \frac{dt'}{\tau}\exp\left(-t/\tau\right)f_o\left(p_z - ea\mathbf{E}t'\right) \tag{17}$$

and $f_o\left(p_z\right)$ is the Fermi-Dirac distribution given as

$$f_o\left(p_z\right) = \frac{1}{\left[\exp\left(-\left(\varepsilon\left(p_z\right)-\mu\right)/k_BT\right)+1\right]} \tag{18}$$

where μ is the chemical potential which ensures the conservation of electrons, k_B is the Boltzmann's constant, T is the absolute temperature in energy units. Substituting Eqs. (17) and (18) into Eq. (15), we obtain an equation for $\Gamma(q)$ which contains Fermi-Dirac integral of the order 1/2 as

$$F_{1/2}\left(\eta_f\right) = \frac{1}{\Gamma(1/2)}\int_0^\infty \frac{\eta_f^{1/2}d\eta}{1+\exp\left(\eta-\eta_f\right)} \tag{19}$$

where $(E_F - E_c)/k_BT \equiv \eta_f$. For nondegenerate electron gas, where the Fermi level is several k_BT below the energy of the conduction band E_c (i.e., $k_BT \ll E_c$), the integral in Eq. (19) approaches $2/\sqrt{\pi}\exp\left(\eta_f\right)$. Eqs. (18) and (19) then simplifies to

$$f_o(p_z) = C\exp\left(-\left[\varepsilon(p_z) - eaE\tau\right]/k_BT\right) \tag{20}$$

where C is the normalization constant to be determined from the normalization condition $\int f(p)dp = n_o$ as

$$C = \frac{3n_oa^2}{2I_o(\Delta_1)I_o(\Delta_2)}\exp\left(\frac{\varepsilon_o - E_F}{k_BT}\right) \tag{21}$$

where n_o is the electron density concentration, T is the absolute temperature in energy units and $I_o(x)$ is the modified Bessel function of zero order.

From the conservation laws, the momentum (p_z) can be deduced from the delta function part of Eq. (15) as

$$p_z = -\frac{\hbar q}{2} + \frac{1}{4a}\arcsin\left(\frac{\omega_q}{12\gamma_o aq}\right) \tag{22}$$

By substituting p_z into the distribution function in Eq. (15), and after some cumbersome calculations yields

$$\begin{aligned}\Gamma_q^{FCNT} = \Gamma_o\Bigg\{&\sinh\left[\Delta_1\cos(3p'a)\sin A\sin\left(\frac{3}{2}a\hbar q\right) + \Delta_2\cos(p'a)\sin B\sin\left(\frac{a}{2}\hbar q\right)\right]\\ &\times\cosh\left[\Delta_1\cos(3p'a)\cos A\cos\left(\frac{3}{2}a\hbar q\right) + \Delta_2\cos(p'a)\cos B\cos\left(\frac{a}{2}\hbar q\right)\right]\\ &-4\Bigg(\Delta_2\sin(p'a)\cos B\sin\left(\frac{a}{2}\hbar q\right) + \Delta_1\cos A\sin(3p'a)\sin\left(\frac{3}{2}a\hbar q\right)\\ &+\Delta_1\Delta_2\sin(p'a)\sin(3p'a)\cos A\cos B\sin\left(\frac{a}{2}\hbar q\right)\sin\left(\frac{3}{2}a\hbar q\right)\Bigg)\\ &\times\sinh\left[\Delta_1\cos(3p'a)\cos A\cos\left(\frac{3}{2}a\hbar q\right) + \Delta_2\cos(p'a)\cos B\cos\left(\frac{a}{2}\hbar q\right)\right]\\ &\times\cosh\left[\Delta_1\cos(3p'a)\sin A\sin\left(\frac{3}{2}a\hbar q\right) + \Delta_2\cos(p'a)\sin B\sin\left(\frac{a}{2}\hbar q\right)\right]\Bigg\}\end{aligned} \tag{23}$$

where $\chi = \hbar\omega_q a/v_s$, Θ is defined to be the Heaviside step function, $\alpha = \omega_q/12\gamma_o aq = \omega_q/6\Delta_1 aq$. In the absence of an external electric field

$$\Gamma_q^{FCNT} = \Gamma_o \left[\sinh \left\{ \Delta_1 \sin\left(\frac{3}{2} a\hbar q\right) \sin A + \Delta_2 \sin\left(\frac{a}{2}\hbar q\right) \sin B \right\} \right.$$
$$\left. \times \cosh \left\{ \Delta_1 \cos\left(\frac{3}{2} a\hbar q\right) \cos A + \Delta_2 \cos\left(\frac{a}{2}\hbar q\right) \cos B \right\} \right] \tag{24}$$

and

$$\Gamma_o = \frac{n_o a^2 \Phi \Lambda^2 q \Theta\left(1-\alpha^2\right)}{48\pi I_o\left(2\gamma_o\beta\right) I_o\left(6\gamma_o\beta\right) \omega_q^2 \sigma v_s \gamma_o \hbar \sqrt{1-\alpha^2}}$$
$$A = \frac{3}{4}\arcsin\left(\frac{\omega_q}{12\gamma_o aq}\right) \quad B = \frac{1}{4}\arcsin\left(\frac{\omega_q}{12\gamma_o aq}\right) \alpha = \frac{\omega_q}{12\gamma_o aq} \tag{25}$$

To compare the result with an undoped SWCNT, we follow the same procedure as that of F-CNT. Using the tight-binding energy dispersion of the p_z orbital which is given as:

$$\varepsilon\left(p_z\right) = \pm\gamma_o \sqrt{1 + 4\cos\left(\frac{\nu\pi}{n}\right)\cos\left(\frac{p_z\sqrt{3}b}{2\hbar}\right) + 4\cos^2\left(\frac{p_z\sqrt{3}b}{2\hbar}\right)} \tag{26}$$

where $\gamma_o = 2.6\,\text{eV}$ is the hopping integral parameter, $b = 0.142\,\text{nm}$ is the C-C bonding distance, and (+) and (−) signs are respectively the conduction and valence band. When $\nu = 0$, the conduction and valence bands cross each other near the Fermi points, $p_F = \pm 2\pi\hbar/3\sqrt{3}b$ giving the metallic nature to the armchair tube. Putting $\nu = 0$, and making the substitution, $p_z = p_z + 3p_o/2\hbar$ in Eq. (26) gives

$$\varepsilon\left(p_z\right) = \pm\gamma_o\left(1 - 2\cos\left(\frac{p_z\sqrt{3}b}{2\hbar}\right)\right) \tag{27}$$

where $p_o = 2p_F = 4\hbar\pi/3\sqrt{3}b \approx 1.7 \times 10^{10}\text{m}^{-1}$ see [24]. Eq. (27) is equivalent to the energy dispersion in Eq. (5) when $n = 1$, which is

$$\varepsilon\left(p_z\right) = \varepsilon_o + \Xi\gamma_o \cos\left(ap_z\right) \tag{28}$$

Using Eq. (15), the absorption in SWCNT is calculated as

$$\Gamma_q^{SWCNT} = \frac{\pi^2\Lambda^2 q^2 \Phi n_o \Theta\left(1-\alpha^2\right)}{4\gamma_o^2 \omega_q^2 v_s \sigma \sin\left(a\hbar q/2\right) I_o\left(2\gamma_o\beta\right)\sqrt{1-\alpha^2}}$$
$$\times \sinh\left\{\beta\hbar\omega_q\right\} \cosh\left\{4\gamma_o\beta\sqrt{1-\alpha^2}\cos\left(\frac{a\hbar q}{2}\right)\right\} \tag{29}$$

where

$$\alpha = \frac{\hbar\omega_q}{4\gamma_o \sin\left(a\hbar q/2\right)} \tag{30}$$

3. Results and discussions

In this formulation, we consider a novel concept of monochromatic acoustic phonon amplification at the THz frequencies regime. Impulsive phonon excitation by a femtosecond optical pulse generates coherent FCNT and SWCNT phonons propagating in the forward and backward direction along the FCNT and SWCNT axis, that is setting up an stationary acoustic wave. Interaction of the propagating acoustic wave with an electrically driven intraminiband transition electron current allows for phonon absorption, connected with electron transitions between states within an electronic miniband. The intravalley or intraminiband character of the electron transport allows for much higher currents than interminiband electron or electron tunneling and thus, a much stronger phonon absorption.

The general expressions for the hypersound absorption in F-CNT (Γ_q^{F-CNT}) and in SWCNT (Γ_q^{SWCNT}) are presented in Eqs. (24) and (29) respectively. In both equations, the absorptions are dependent on the frequency (ω_q), the acoustic wavenumber (q), and temperature (T) as well as other parameters such as the inter-atomic distances, the velocity of sound (v_s) and the deformation potential (Λ). In both expressions (see Eqs. (24) and (29)) a transparency window is observed: for F-CNT is $\omega_q \gg 12\gamma_o aq$; and for SWCNT is $\omega_q \gg \gamma_o \sin\left(\frac{1}{2}a\hbar q\right)/\hbar$. These are the consequence of conservation laws. The Eqs. (24) and (29), are analyzed numerically with the following parameters used: $\Lambda = 9\,\text{eV}$, $q = 10^5\,\text{cm}^{-1}$, $\omega_q = 10^{12}\,\text{s}^{-1}$, $v_s = 5 \times 10^3\,\text{m/s}$, $\Phi = 10^4\,\text{Wb/m}^2$, and $T = 45\,\text{K}$. The results are graphically plotted (see **Figures 4–7**). **Figure 4** shows the dependence of the sound absorption coefficient on the frequency (ω_q) for varying q. In both graphs, the absorption is initially high but falls off sharply and then changes slowly at high values of ω_q. Increasing the values of q correspondingly increases the obtained graph in both doped F-CNT and undoped SWCNT though the magnitude of absorption obtained in SWCNT exceeds that of F-CNT, that is, $|\Gamma_q^{SWCNT}| > |\Gamma_q^{F-CNT}|$. This is in accordance with the work of Jeon et al. [19]. In **Figure 2**, the graph increases to a maximum point then drops off. It then changes again slowly at high q for both undoped SWCNT and doped F-CNT. By increasing the temperature, the amplitude of the graphs reduces. For $T = 45\,K$, the maximum absorption in $\Gamma_q^{SWCNT} = 8.2 \times 10^4$ whilst that of $\Gamma_q^{F-CNT} = 2867$ which gives the ratio of the absorption $\frac{\Gamma_{(SWNT)}}{\Gamma_{(F-CNT)}} \approx 29$, whilst at $T = 55\,K$, $\frac{\Gamma_{(SWNT)}}{\Gamma_{(F-CNT)}} \approx 9$ and at $T = 65\,K$, we had $\frac{\Gamma_{(SWNT)}}{\Gamma_{(F-CNT)}} \approx 2$. Clearly, we noticed that the ratio decreases with an increase in temperature. The nonlinear behavior in **Figure 5** is as a result of the fact that, increasing temperature increases the scattering process in the material. The majority of electrons in this case acquire a higher velocity, shorter collision time, and higher energy. This energetic electrons, which are the majority undergo inter-mini-band transition (tunneling) allowing only a handful to undergo intra-mini-band transition. This allows only the few intra-mini-band electrons to interact with the copropagating phonons

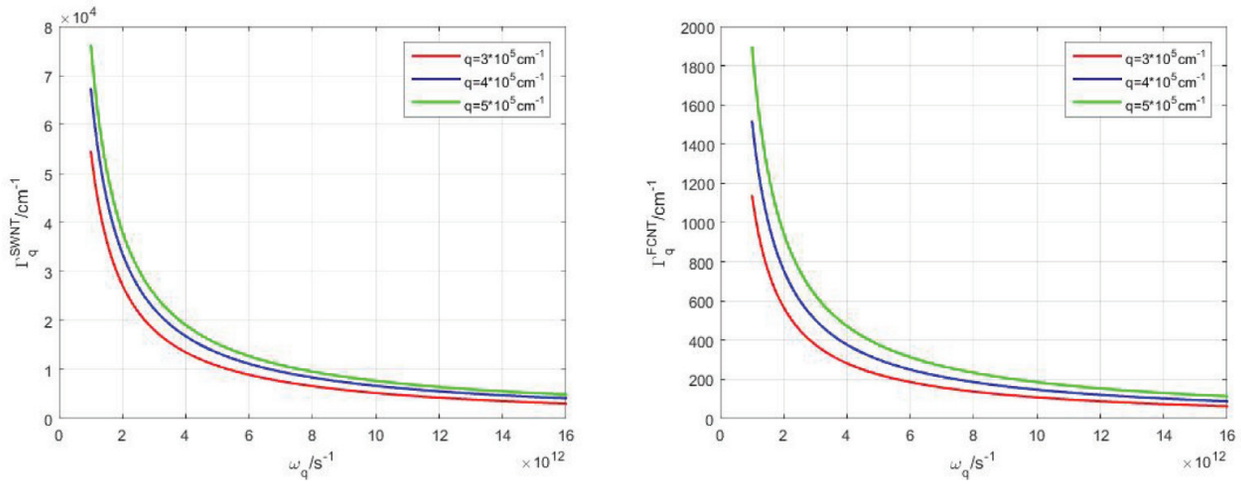

Figure 4. Dependence of Γ_q on ω_q (left) for an undoped SWCNT, and (right) for a F-CNT by varying q at $T = 45$ K.

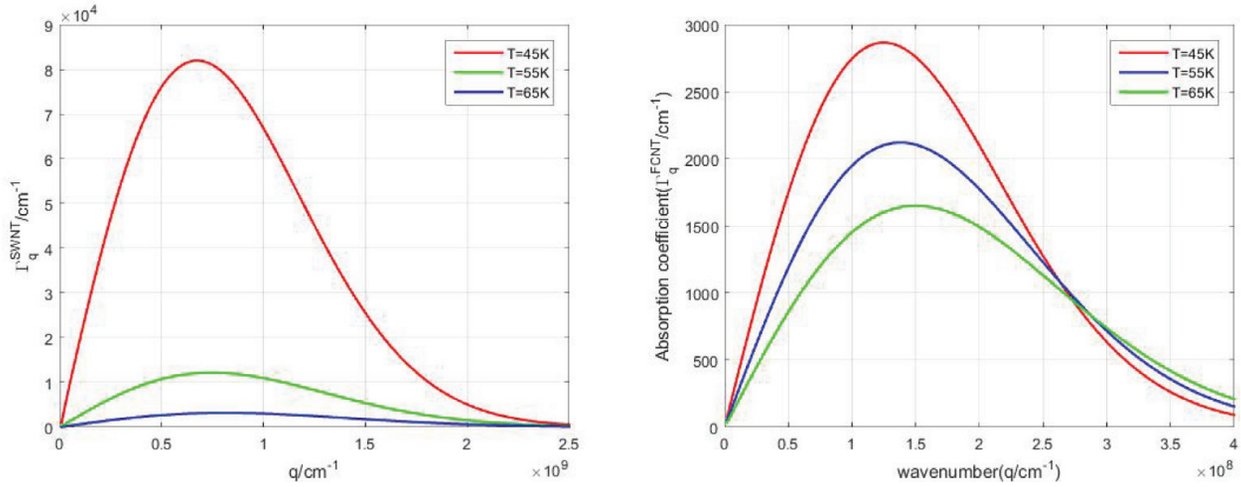

Figure 5. Dependence of Γ_q on q (left) for undoped SWCNT and (right) for doped F-CNT at $T = 45, 55, 65$ K.

leading to a decrease in absorption of the acoustic phonons. To aid a better understanding of the comparison between the absorption obtained in both SWCNT and F-CNT, a semilog plot is presented in **Figure 6**, which clearly shows that the undoped SWCNT absorbs more than the doped F-CNT. This can be attributed to the fact that the presence of F-CNT atoms leads to chemical activation of a passive surface CNT by adding additional electronic band structure and altering the carbon π-bonds around the Fermi level in a non-linear manner thus forming a band structure of width two periods [22]. As Flourine is highly electronegative it thus weakens the walls of the CNT as it approaches it. The π-electrons attached to the Flourine which causes less free charge carriers to interact with the phonons. Current researches have predicted sp^2 bonding charge change to sp^3 by F-functionlization [25–27]. This bonding charge change would reduce the density of free carriers, consequently leading to the magnitude reduction of the absorption [22] (**Figures 4–6**).

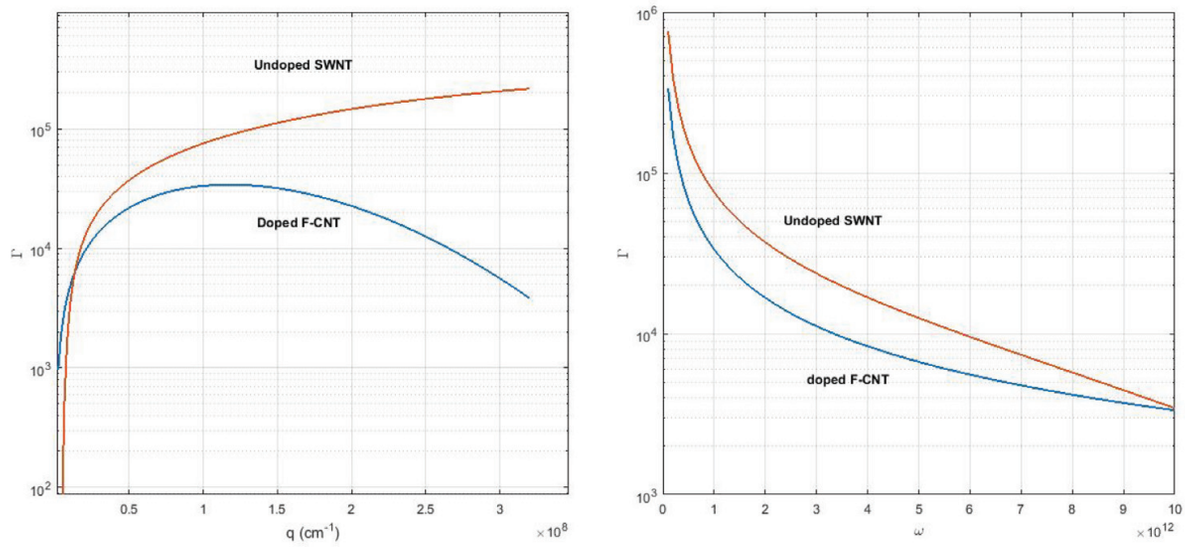

Figure 6. Semilog plot of Γ_q dependence on q and ω_q for doped F-CNT and undoped SWCNT.

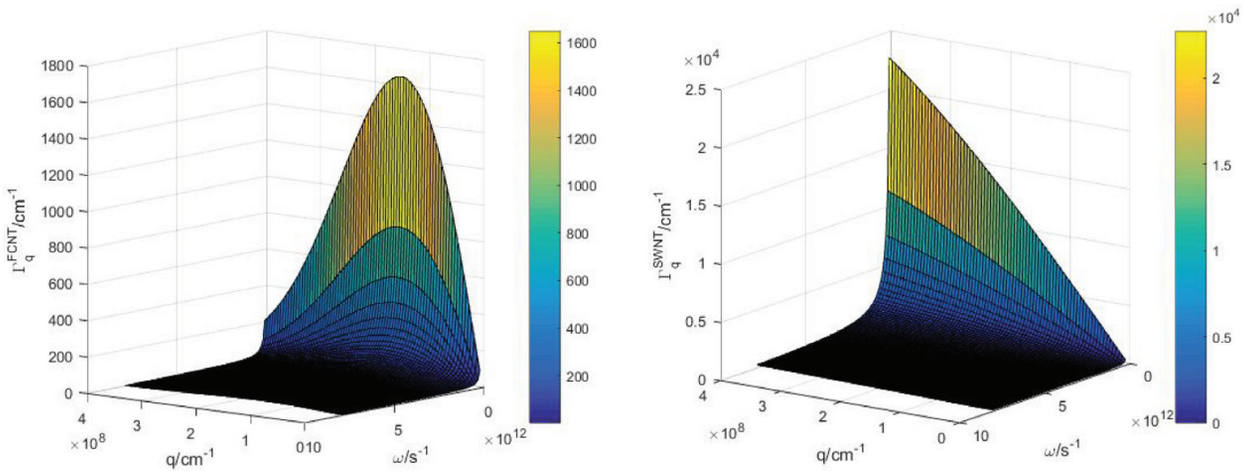

Figure 7. A three dimensional plot of Γ_q dependence on q and ω_q for doped and undoped SWCNT.

In order to put our observations in perspective, we display **Figures 4** and **5** in a three-dimensional behavior of the sound coefficient as a function of the frequency (ω_q) and the wavevector q (**Figure 7**).

4. Conclusion

Theoretical investigation of strong absorption of coherent acoustic phonons in an FCNT and SWCNT at low temperature utilizing the Boltzmann's transport equation is carried out in the regime $ql \gg 1$. The absorption coefficient obtained is highly nonlinear and depends on the

stimulated absorption of acoustic phonons by electrically determined electrons experiencing intraminiband transport. The study is appropriate and furthermore considers a strong absorption of energized FCNT and SWCNT phonons. The Flourine doping affects the absorption properties of F-CNT, whereas SWCNT absorbs better than the F-CNT as was observed by Jeon et al. [19]. The phonons absorbed in this study have THz frequencies with wavelengths in the nanometer run, and takes into account examinations with high spatial determination, e.g., in phonon filters, spectroscopy (phonon spectrometer), microbiology, micro-nanoelectronic gadgets, tetrahertz adjustment of light, nondestructive testing of microstructures, and acoustic examination.

Author details

Daniel Sakyi-Arthur[1]*, S. Y. Mensah[1], N. G. Mensah[2], Kwadwo A. Dompreh[1] and R. Edziah[1]

*Address all correspondence to: daniel.sekyi-arthur@stu.ucc.edu.gh

1 Department of Physics, College of Agriculture and Natural Sciences, University of Cape Coast, Ghana

2 Department of Mathematics, College of Agriculture and Natural Sciences, University of Cape Coast, Ghana

References

[1] Shinokita K, Reimann K, Woerner M, Elsaesser T, Hey R, Flytzanis C. Strong amplification of coherent acoustic phonons by Intraminiband currents in a semiconductor Superlattice. Physical Review Letters. 2016;**116**(7):075504

[2] Gokhale VJ, Shim Y, Rais-Zadeh M. Observation of the acoustoelectric effect in gallium nitride micromechanical bulk acoustic filters. In: Frequency Control Symposium (FCS), 2010 IEEE International. IEEE; 2010. pp. 524-529

[3] Mensah SY, Allotey FKA, Adjepong SK. Acoustomagnetoelectric effect in a superlattice. Journal of Physics: Condensed Matter. 1996;**8**(9):1235

[4] Dompreh KA, Mensah SY, Abukari SS, Edziah R, Mensah NG, Quaye HA. Acoustomagnetoelectric effect in Graphene Nanoribbon in the presence of external electric and magnetic fields. Nanoscale Systems: Mathematical Modeling, Theory and Applications. 2014;**4**(1)

[5] Sharma GS, Skvortsov A, MacGillivray I, Nicole K. Acoustic performance of gratings of cylindrical voids in a soft elastic medium with a steel backing. The Journal of the Acoustical Society of America. 2017;**141**(6):4694-4704

[6] Ge H, Yang M, Ma C, Ming-Hui L, Chen Y-F, Fang N, Ping S. Breaking the barriers: Advances in acoustic functional materials. National Science Review. 2017

[7] Mensah SY, Allotey FKA, Adjepong SK. The effect of a high-frequency electric field on hypersound amplification in a superlattice. Journal of Physics: Condensed Matter. 1994; **6**(19):3479

[8] Mensah SY, Allotey FKA, Mensah NG, Elloh VW. Amplification of acoustic phonons in a degenerate semiconductor superlattice. Physica E: Low-dimensional Systems and Nanostructures. 2003;**19**(3):257-262

[9] Nunes OAC, Fonseca ALA. Amplification of hippersound in graphene under external direct current electric field. Journal of Applied Physics. 2012;**112**:043707

[10] Dompreh KA, Mensah NG, Mensah SY. Amplification of hypersound in graphene with degenerate energy dispersion. arXiv preprint arXiv. 2015;**1503**:07360

[11] Miseikis V, Cunningham JE, Saeed K, ORorke R, Davies AG. Acoustically induced current flow in graphene. Applied Physics Letters. 2012;**100**(13):133105

[12] Bandhu L, Nash GR. Temperature dependence of the acoustoelectric current in graphene. Applied Physics Letters. 2014;**105**(26):263106

[13] Dompreh KA, Mensah NG, Mensah SY, Abukari SS, Sam F, Edziah R. Hypersound absorption of acoustic phonons in a degenerate carbon nanotube. arXiv preprint arXiv. 2015;**1502**:07636

[14] Dompreh KA, Mensah NG, Mensah SY, Sam F, Twum AK. Acoustoelectric effect in degenerate carbon nanotube. arXiv preprint arXiv. 2015;**1504**:05484

[15] Reulet B, Kasumov AY, Kociak M, Deblock R, Khodos II, Gorbatov YB, Volkov VT, Journet C, Bouchiat H. Acoustoelectric effects in carbon nanotubes. Physical Review Letters. 2000;**85**(13):2829

[16] Ebbecke J, Strobl CJ, Wixforth A. Acoustoelectric current transport through single-walled carbon nanotubes. Physical Review B. 2004;**70**(23):233401

[17] Amekpewu M, Abukari SS, Adu KW, Mensah SY, Mensah NG. Effect of hot electrons on the electrical conductivity of carbon nanotubes under the influence of applied dc field. The European Physical Journal B. 2015;**88**(2):1-6

[18] Mensah SY, Allotey FKA, Mensah NG, Nkrumah G. Differential thermopower of a CNT chiral carbon nanotube. Journal of Physics: Condensed Matter. 2001;**13**(24):5653

[19] Jeon T-I, Son J-H, An KH, Lee YH, Lee YS. Terahertz absorption and dispersion of fluorine-doped single-walled carbon nanotube. Journal of Applied Physics. 2005;**98**(3):34316

[20] Hattori Y, Touhara H. Fluorination-defluorination and fluorine storage properties of single-wall carbon nanotubes and carbon nanohorns. New Fluorinated Carbons: Fundamentals and Applications. 2017:113-133

[21] Zhang KS, Pham D, Lawal O, Ghosh S, Gangoli VS, Smalley P, Kennedy K, et al. Overcoming catalyst residue inhibition of the functionalization of single-walled carbon nanotubes via the Billups-birch reduction. ACS Applied Materials & Interfaces. 2017;**9**(43):37972-37980

[22] Sadykov NR, Kocherga EY, Dyachkov PN. Nonlinear current in modified nanotubes with exposure to alternating and constant electric fields. Russian Journal of Inorganic Chemistry. 2013;**58**(8):951-955

[23] Mensah SY, Allotey FKA, Mensah NG. Nonlinear acoustoelectric effect in a semiconductor superlattice. Journal of Physics: Condensed Matter. 2000;**12**(24):5225

[24] Hasan S. Electron phonon interaction in carbon nanotube devices [PhD dissertation]. West Lafayette: Purdue University; 2007

[25] Chen J, Yan L. Recent advances in carbon nanotube-polymer composites. Advances in Materials. 2017;**6**(6):129

[26] Bauschlicher CW, So CR. High coverages of hydrogen on (10, 0), (9, 0) and (5, 5) carbon nanotubes. Nano Letters. 2002;**2**(4):337-341

[27] Sharma B, Kar R, Pal AR, Shilpa RK, Dusane RO, Patil DS, Suryawanshi SR, More MA, Sinha S. Role of hydrogen diffusion in temperature-induced transformation of carbon nanostructures deposited on metallic substrates by using a specially designed fused hollow cathode cold atmospheric pressure plasma source. Journal of Physics D: Applied Physics. 2017;**50**(15):155207